Pre-clinic study of radiopharmaceutical for Covid-19 inactivation: Dose distribution with Monte Carlo Simulation

Ozge Kilicoglu [a,b,*], Umit Kara [c,d], Emre Ozgenc [e], Evren Gundogdu [e]

[a] Vocational School of Health Services, Marmara University, Kartal, Istanbul, Turkey
[b] Radiation Laboratory, University of Notre Dame, Notre Dame, IN, 46556-5670, USA
[c] Suleyman Demirel University, Vocational School of Health Services, Medical Imaging Department, Isparta, Turkey
[d] Suleyman Demirel University Research and Practice Hospital, Department of Radiology Quality and Radiation Protection, Isparta, Turkey
[e] Department of Radiopharmacy, Faculty of Pharmacy, Ege University, Bornova, Izmir, Turkey

ARTICLE INFO

ABSTRACT

Monte Carlo simulation method and Nuclear Medicine MIRD method were used to evaluate the effect of radiopharmaceuticals on Covid-19 disease. The mean absorbed organ dose in the target organ and gamma radiation emitter attenuation properties such as linear attenuation coefficients, energy absorption build-up factors (EABF), exposure build-up factors (EBF), and relative dose distributions (RDD) were examined. The results showed that radiopharmaceuticals containing gamma radiation emitters which are densely ionizing charged particles induced membrane damage and produced protein damage.

1. Introduction

The coronavirus pandemic of 2019–2020 is caused by severe acute respiratory syndrome-2. Angiotensin-converting enzyme 2 (ACE2) is not commonly found in the bloodstream but is expressed in many tissues and organs such as the cardiovascular system and the lungs. It regulates blood pressure in the body and is therefore targeted for the treatment of hypertension. The spike glycoprotein of SARS-CoV2 binds to the ACE2 receptor in the membranes of cells and SARS-CoV2 invades host cells. Therefore, ACE2 is also referred to as the SARS-CoV2 receptor. ACE2 regulates the activity of the protein angiotensin II (Ang II), which causes increased blood pressure, blood vessel damage, and inflammation. When SARS-CoV2 binds to the ACE2 receptor, it prevents ACE2 from functioning. In covid patients, it causes increased inflammation and heart and lung damage (Gheblawi et al., 2020). ACE2 enzyme, a host receptor for SARS-CoV-2 which enters into cells, is a transmembrane metalloproteinase. The binding of SARS-CoV-2 to ACE2 and its absorption of ACE2 has shown to down-regulate the functions of this enzyme, and it leaves Ang II/AT1R actions unbalanced. (Zhou et al., 2020).

Previous studies have reported that radiation at a very high dose (10 kGy) and low LET inactivates MERS-CoV and SARS-CoV viruses. In addition, the use of low doses has been reported to cause viral reactivation for some viruses (Salomaa et al., 2020). Lung cells are very

sensitive to radiation. The risk of complications in healthy lung tissue when treating lung neoplasms, breast or Hodgkin's disease has been an important limiting step in determining treatment dose (Jain and Berman 2018). This is very important because SARS-CoV-2 viruses show uptake at ACE2 receptors in the lung. Lung tissue is extremely sensitive to radiation and low-dose radiation should be used to inactivate SARS-CoV-2 viruses (Prasanna et al., 2020; Ameri et al., 2021). However, it is not known whether the use of low-dose radiation causes the reactivation of SARS-CoV-2 viruses. The dose of radiation required to inactivate SARS-CoV-2 viruses is of great importance. In this study, it is shown that the maximum radiation dose that can be used to kill SARS-CoV-2 viruses is within the limits that are accepted as safe for humans, taking into account the potential risks of radiation exposure (Prasanna et al., 2020).

Monte Carlo Simulation with low-dose radiation has been studied as a possible inactivation method for Covid-19 patients. However, there is still a lack of connection and knowledge gap in the literature on the biological and clinical effects of the use of gamma radiation since the clinical use of gamma radiation emitter is not a part of the inactivation method in most cancer research centers. In this sense, the clinical basis of the hypothesis is limited. Three case series were published in 1943 on virus-associated patients with interstitial pneumonia (without the involvement of bacteria in the sputum). The scientific analysis and discussion of this subject are therefore important and relevant. One study used doses of 0.35–0.9 Gy for 130–150 kV X-rays in the affected
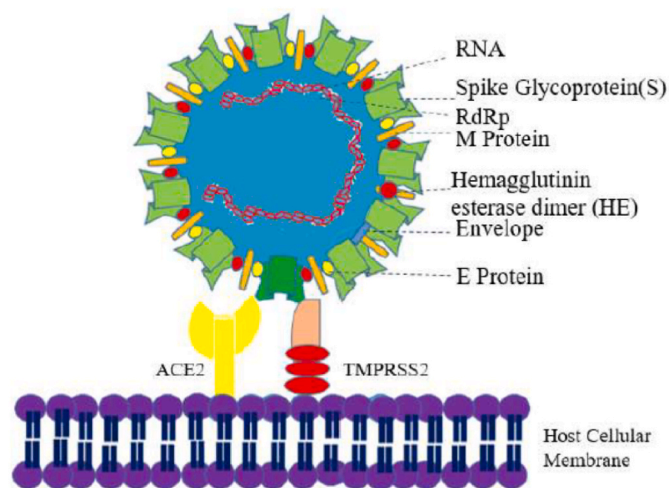

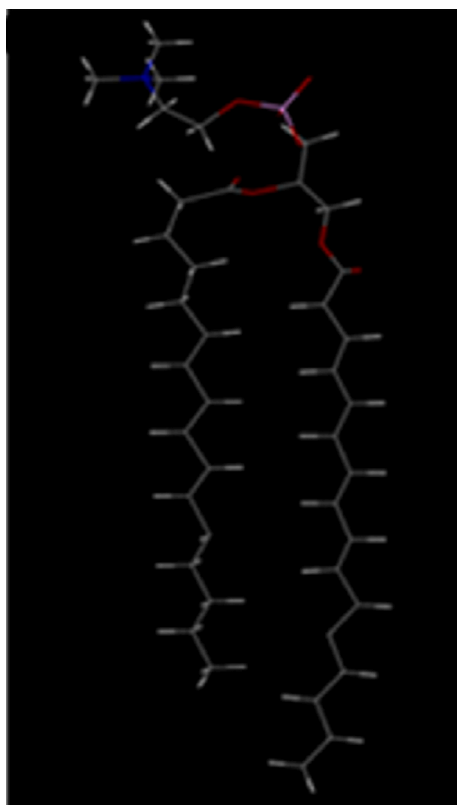**Fig. 1.** Coronavirus structure with proteins and lipid layer.

Fig. 2a. The atomic structure of the DPPC molecule

lung region without establishing a control group (Little et al., 2021). In retrospect, the first study on the radiation inactivation method for viral diseases pointed out that there was a reduction in symptoms when the patient received the inactivation method early. Initially, Monte Carlo simulations will be performed on the interaction of radiation with the virus both in vitro and in vivo to demonstrate the effects of low-dose radiation on the virus. Low-dose radiation is thought to polarize macrophages to the M2 phenotype and reduce the production of inflammatory cytokines. In our research, the potential risks of radiation exposures are considered but the maximum dose to kill the coronaviruses remains still within the limits considered safe for humans.

The effects of X-rays on pneumonia studies are focused on the anti-inflammatory effects. Nasir et al. in their study cited low-dose lung

irradiation in COVID-19 as a solution that could be an auxiliary treatment by improving interstitial pneumonia PaO2/FiO2 (Nasir et al., 2021).

In addition, the review showed low doses from kilovoltage X-rays reduced pneumonia mortality from roughly 30 percent to 10 percent on average and radiation doses reported were generally in the 20 few hundred roentgen range, which given the attenuation through the chest wall would likely have resulted in mean lung doses in the tens to <100 cGy range (Oppenheimer 1943). Pneumonia occurs as an inflammatory immune response when the alveoli become inflamed. In a viral infection, viruses trigger immune cells to synthesize proinflammatory cytokines and chemokines to provoke an immune response. Older studies indicate induction of an anti-inflammatory phenotype. They are induced by low radiation doses as a potential explanation. The administration of 200 cGy doses in proinflammatory effects that trigger common toxicity and radiation therapy, and more recent studies show low doses, such as (<100 cGy) provoke anti-inflammatory properties. Decreasing levels of proinflammatory cytokines such as IL-1b inhibit leukocyte uptake. Therefore, an LRT or radiopharmaceutical treatment of 30–100 cGY to a patient's lungs COVID-19 pneumonia can reduce inflammation and alleviate life-threatening symptoms (Kirkby and Mackenzie 2020).

Unlike these previous studies, present studies demonstrate findings regarding the role of X-rays in the treatment of pneumonia. Our goal with Monte Carlo simulation is to see if pre-clinical radiopharmaceuticals can be used in this treatment, especially before moving on to animal studies. Within the context of the current COVID-19 pandemic and an ongoing global health crisis, this research now merits contemporary research.

With the help of molecular imaging technology, radiopharmaceutical therapy could be applied at the molecular and cellular levels in humans (Terán et al., 2005). Molecular imaging technology with radiopharmaceuticals has already been used for a wide variety of applications such as drug development, pharmacokinetic studies, clinical diagnosis, and therapy of cancers (Gutfilen and Valentini 2014). In recent years, there is significant progress in the development of radiopharmaceuticals for nuclear imaging and the inactivation of some viruses. The success of molecular imaging and inactivation of viruses is assumed to be dependent on the selective accumulation of diagnostic or therapeutic radiopharmaceuticals in the region of interest. Significant efforts are still being made in both pre-clinical and clinical trials to improve the precision of selective radioisotopes. The design of the radiopharmaceutical products and the selection of the best application method are very critical and complex refinements for a better inactivation result (Qin 2015). By offering more successful therapies, the development and implementation of new radiopharmaceuticals will offer ground-breaking solutions to clinical problems (Masur et al., 2014; Lederman et al., 2016).

These reasons encouraged researchers to continue evaluating the effectiveness of radioimmunotherapy (RIT) in the inactivation of infectious diseases because many microorganisms divide much more quickly than mammalian cells, and the radionuclides were chosen for the infection's inactivation and they should be able to release radiation in a short time. The Technetium-99 m (Tc-99m) has gamma emitter radiation, available half-life, 140 keV of photon energy, and was selected in this study. Furthermore, the effect of Tc-99m on covid-19 was evaluated by using dose distribution and Monte Carlo Simulation.

2. Materials and methods

Coronavirus (Covid-19) is a lethal strain of RNA viruses such as Severe Acute Respiratory Syndrome (SARS) and Middle East Respiratory Syndrome (MERS) (Channappanavar and Perlman 2017). However, the SARS-CoV-2 virus is much more infectious and lethal than MERS and SARS. Viruses typically require a primary receptor to bind and effectively invade host cells. Coronavirus also binds an enzyme called angiotensin-converting enzyme 2 (ACE 2) to enter cells attached to the
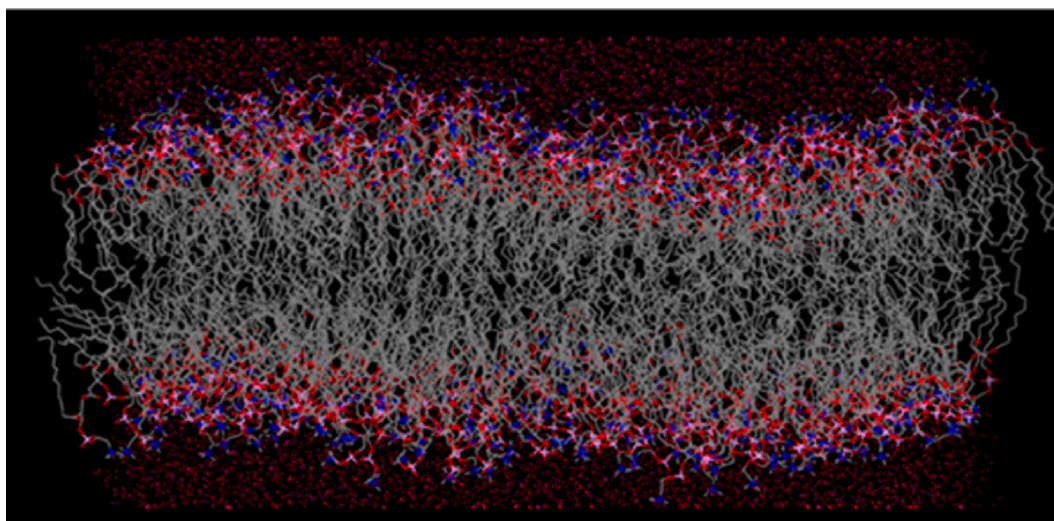
Fig.2b. Lipid bilayer of the DPPC with water around.

Table 1
Chemical compositions (wt %) of Lipid Layer (DPPC) and Spike Protein (S).

Atom Type	Lipid Layer (DPPC)	Spike protein (S)
C	65.48	52.38
H	10.91	9.51
O	17.46	21.55
N	1.91	15.59
P	4.23	–
S	–	0.97
Density(g/cm^3)	0.95	1.30

membrane. These enzymes are especially present in the intestine, kidney, and blood vessels as well as wrapping lung (epithelial) cells (Wan et al., 2020).

As far as the outer structure of Covid-19 containing spike protein and lipid structure is vulnerable to inactivation of viruses and that can be obtained by radiopharmaceutical containing gamma radiation emitter. The external structure of the virus interacting with applied radiopharmaceuticals can be helpful for the inactivation of the virus (Mettler Jr and Guiberteau 2012; Ziessman and O'Malley 2013). Computing a Monte Carlo-based code simulation with Tc-99m can be an alternative inactivation of Covid-19.

Radiopharmaceuticals can be used in the therapy and diagnosis of many diseases. They have tissue destruction effect by transferring radiation energy to desired tissues. The effect of radiation on the tissue is expressed as the amount of radiation absorbed in Gray (Gy). In radiation administration by using radiopharmaceuticals, there is a relationship between radiation dose-response in terms of cell death and survival rate. Measuring the amount of radiation absorbed in the targeted tissue is the main point for the inactivation of the virus. In this respect, radiopharmaceutical administration based on the inactivation virus can be considered a natural part of this approach.

There is a lot of conceptual confusion in the use of the term "dose" in the literature. This concept is generally the amount of radiation in Gy in the system of international units. However, the term "dose" used by clinicians is used instead of mCi or GBq, which is the activity unit applied. For a dosimetry approach, these expressions must be used correctly. Medical Internal Radiation Dosimetry (MIRD) formulations are often used for dosimetric examinations in clinical applications. The MIRD method is based on dose calculation on the standard size human body and its organ models. In this method, the amount of dose absorbed in the target organs is calculated based on radioactivity in the source organs. In this study, we used the Visual Monte Carlo Program (VMC);
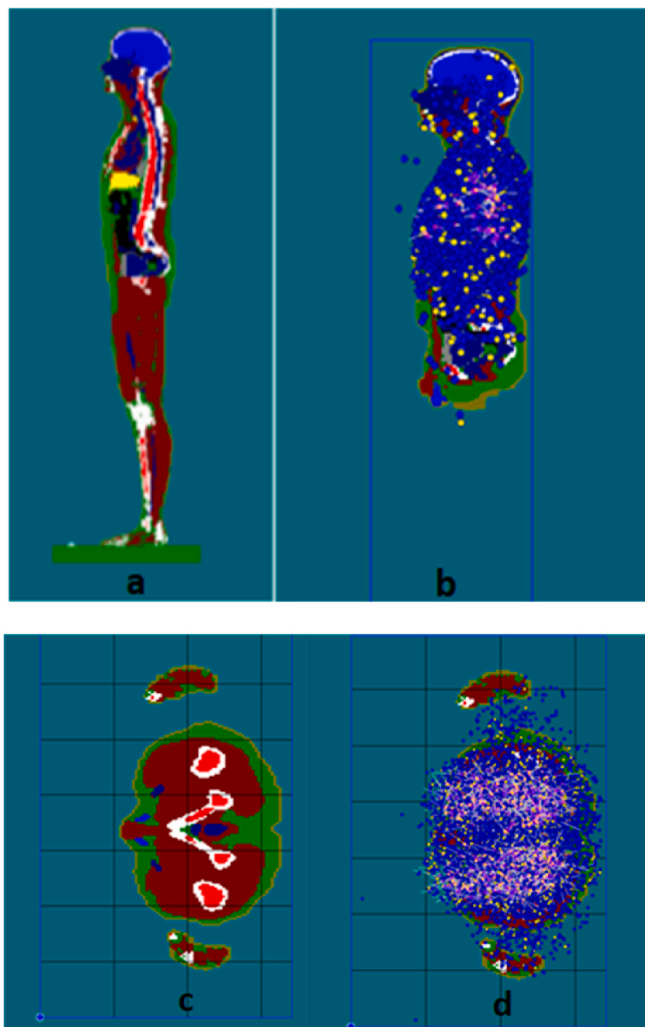

Fig. 3. Simulation geometry a-b) inside view, c-d) top view (Technetium-99m) source a-c) Tc-99-free used simulation; b-d) Tc-99 used simulation.

Table 2
The mass attenuation coefficients (cm^2/g) values derived from MATLAB code and WinXCOM program for Lipid Layer (DPPC) and Spike Protein (S).

| Lipid Layer (DPPC)				Spike protein (S)			
MeV	WinXCOM	Matlab	% Dev	MeV	WinXCOM	Matlab	% Dev
0.015	1.4380	1.398048	0.0286	0.015	1.1970	1.164815	0.0276
0.02	0.7192	0.717365	0.0026	0.02	0.6145	0.613135	0.0022
0.03	0.3505	0.353987	0.0099	0.03	0.3179	0.31331	0.0146
0.04	0.2575	0.256887	0.0024	0.04	0.2426	0.242126	0.0020
0.05	0.2209	0.22122	0.0014	0.05	0.2124	0.212632	0.0011
0.06	0.2019	0.202434	0.0026	0.06	0.1962	0.196627	0.0022
0.08	0.1814	0.181175	0.0012	0.08	0.1780	0.17772	0.0016
0.1	0.1691	0.169201	0.0006	0.1	0.1665	0.166558	0.0003
0.15	0.1495	0.149977	0.0032	0.15	0.1476	0.148073	0.0032
0.2	0.1363	0.136195	0.0008	0.2	0.1346	0.134584	0.0001
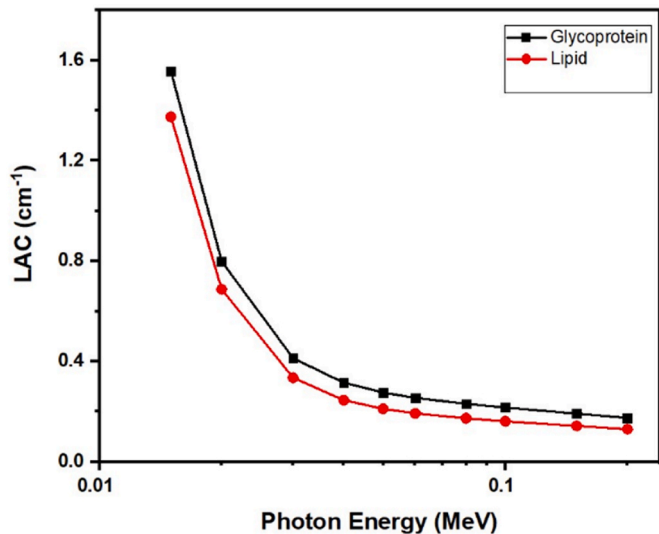
Fig. 4. Linear attenuation coefficient (LAC) values as a function of the photon energy of Glycoprotein and Lipid layers.
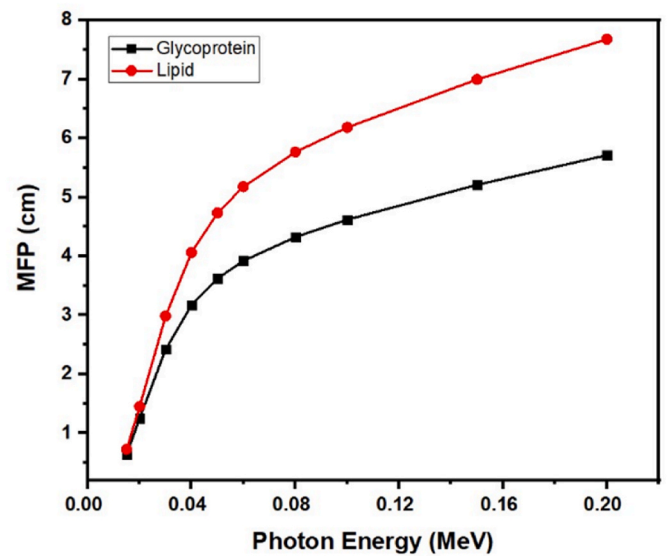

Fig. 6. Mean free path (MFP) values as a function of the photon energy of Glycoprotein and Lipid layers.
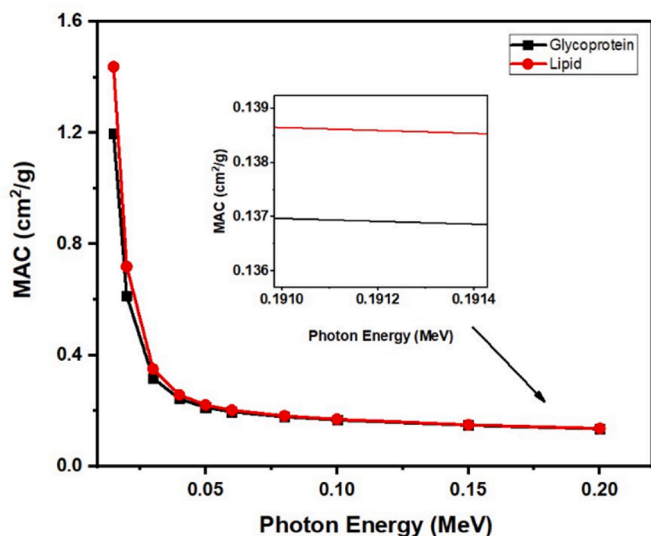

Fig. 5. Mass attenuation coefficient (MAC) values as a function of the photon energy of Glycoprotein and Lipid layers.

VMC is computer software that easily simulates the radiation interaction of the human body with sources such as gamma radiation, which is used clinically. VMC is a Monte Carlo code specially designed for voxel geometries and it is written in Visual Basic. The simulation works on internal or external dose calculations during occupational exposure in 0.02–1.5 MeV as energies of radionuclides. The lung tissue is targeted in this study and the lung volume is used to calculate by multiplying it with a density value of 0.3 g/cm^3 and converting it into mass and MIRD method using VMC simulation defining the mean absorbed dose (D) to a target region (r T) for a time-independent system as shown Equation (1):

$$D(rT,TD) = \sum rS \sim A(rS,TD)S(rT \leftarrow rS) \ [Gy] \tag{1}$$

where $\tilde{A}(r_S, T_D)$ is the time-integrated or cumulated activity (i.e., the total number of disintegrations in source region r_S over the integration period T_D (Mattsson et al., 2015). This integration period is in hours and T_D is normally set to ∞. $S(r_T \leftarrow r_S)$ is the mean absorbed dose in the target tissue per nuclear transformation in the source region and is defined as Equation (2):

$$S(rT \leftarrow rS) = \sum i \Delta i \Phi(rT \leftarrow rS,Ei) \ [Gy/Bq] \tag{2}$$

where $\Phi(r_T \leftarrow r_S, E_i)$ is the SAF value (i.e., the fraction of the E_i emitted in source region r_S to the target tissue r_T divided by the mass of the target tissue in kilograms) of the i-th emitted radiation of the radionuclide and $\Delta_i = E_i Y_i$ (the product of Y_i, the yield, and E_i is the mean energy (or part of the energy distribution for β-decay) of the i-th nuclear transition of the radionuclide in joules (Eckerman 2008; Bolch et al., 2016; Mattsson et al., 2015).

In addition to the MIRD method, this study includes and simulates mass attenuation coefficient with the WinxCOM program and calculated
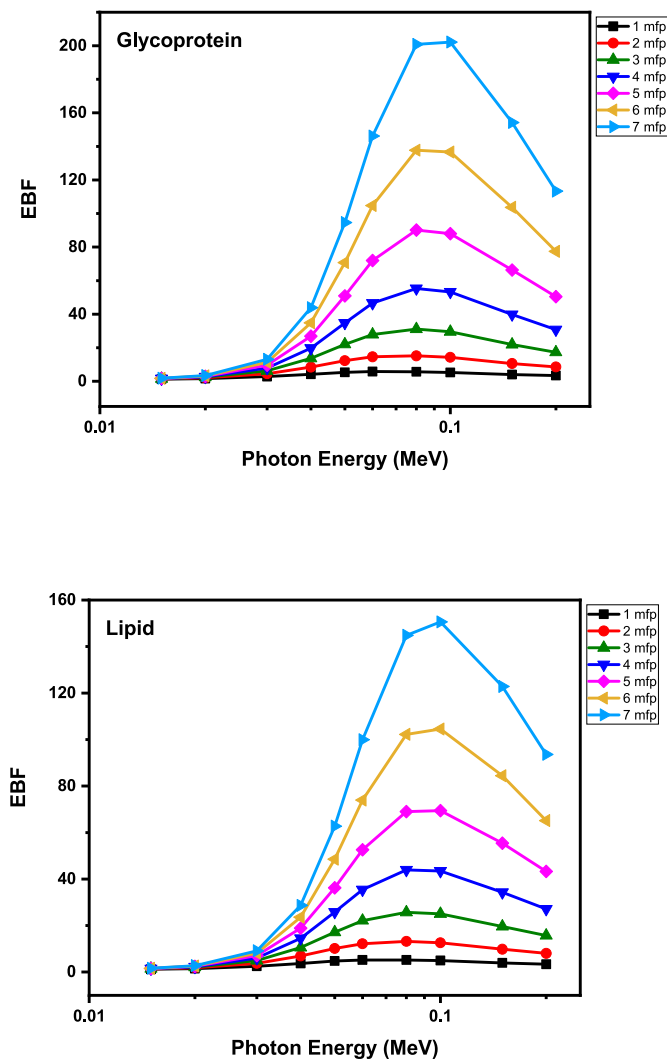
Fig. 7. Exposure buildup factor (EBF) values as a function of the photon energy of Glycoprotein and Lipid layers.

Fig. 8. Energy absorption buildup factor (EABF) values as a function of the photon energy of Glycoprotein and Lipid layers.

radiation interaction parameters. The surface structure of Covid-19 with the data given below; a spike glycoprotein (S), hemagglutinin-esterase dimer (HE), a membrane glycoprotein (M), an envelope protein (E), an RNA dependent-RNA polymerase (RdRp) and RNA as seen in Fig. 1 (Vardhan and Sahoo 2020). The spike protein (S) depicted (PDB ID: 6VSB) in Fig. 1 is the protein that allows the virus to attach to and fuse with a host cell's membrane.

Dipalmitoylphosphatidylcholine (DPPC) molecule (Fig. 2a) is one of the most studied phospholipids which consists of two palmitic acids attached to a phosphatidylcholine head-group and plays an important role in the study of liposomes and human cell bilayers (Fig. 2b). Mass weight percentages of the Covid-19 spike protein (S) and lipid layer (DPPC) were calculated with the Materials Studio program and given in Table 1. The density of DPPC lipid bilayers is predicted as approximately 0.95 g/cm^3 (Miyoshi et al., 2014) and the buoyant density of spike protein (S) is taken at approximately 1.3 g/cm^3 (Mazzone 1998; Padilla-Sanchez 2020).

Herein, the gamma radiation emitters, molecular mechanisms, transporter, and trapping mechanism uptake were designed by VMC Monte Carlo Simulation in Fig. 3.

MATLAB is a mathematical and scientific computing software kit developed by MathWorks. It was defined by Lambert's Beer Law given by the equation below. The Image Processing Toolbox in MATLAB allows for matrix calculation, method implementation, simulation,
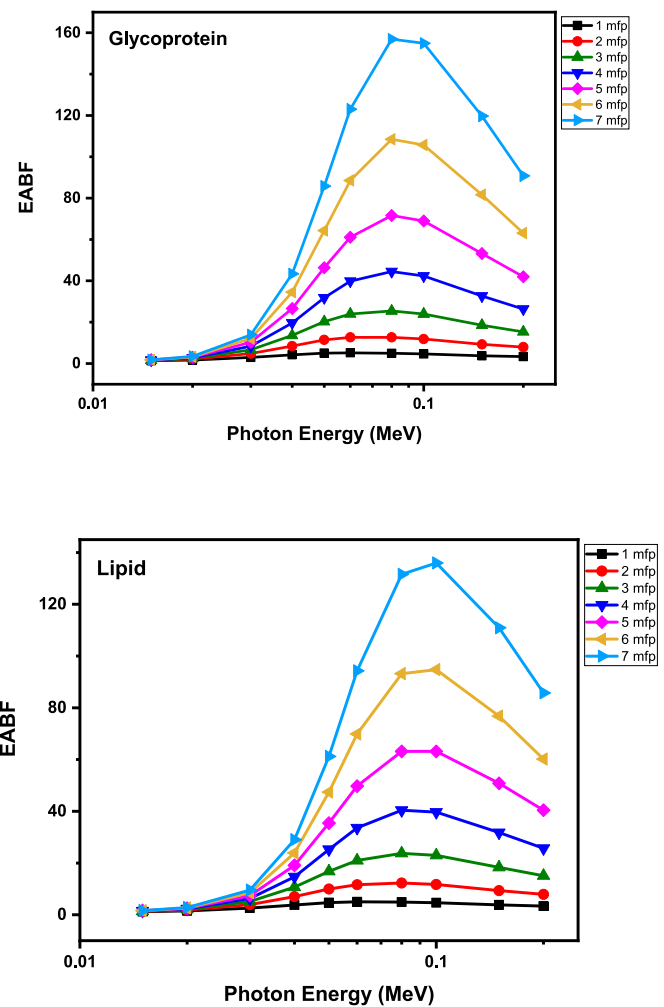
function design, data, signal, and image transform. All of MATLAB's functions for presenting any functional analysis are required after the acquisition of an image. The majority of toolbox functions are written in the open MATLAB language, allowing users to inspect algorithms, restrict source code, and build system functions (Lyra et al., 2011). In this study, we have covered the mass attenuation coefficient calculated by the Monte Carlo Simulation with MATLAB codes, and the WinxCOM program; these calculations are recorded **in** Table 2. These procedures for computing parameters are important when it comes to radiation shielding and attenuation studies (Kilicoglu, O. and Mehmetcik, H. 2021).

Covid-19 layers were designed in MATLAB with Monte Carlo Simulation codes and their factor of gamma-radiation emitter' attenuation is investigated for the patients' needs and nuclear medicine administration. The theoretical mass attenuation coefficient of virus layers can be calculated for the energy region by using the WinxCOM program (Berger et al., 2010; Gerward et al., 2004) and MATLAB code (see Eq. (3)).

$$I \, / \, Io = exp[-(\mu \, / \, \rho)x] \qquad (3)$$

$$(\mu \, / \, \rho) = \left[\sum_i W_i(\mu \, / \, \rho)_i \right] \qquad (4)$$

In equation (3), I_0 and I are the main and attenuated photons, with their intensities. This equation represents a generic formulation of radiation attenuation by incorporating the primary (I_o) and secondary (I)
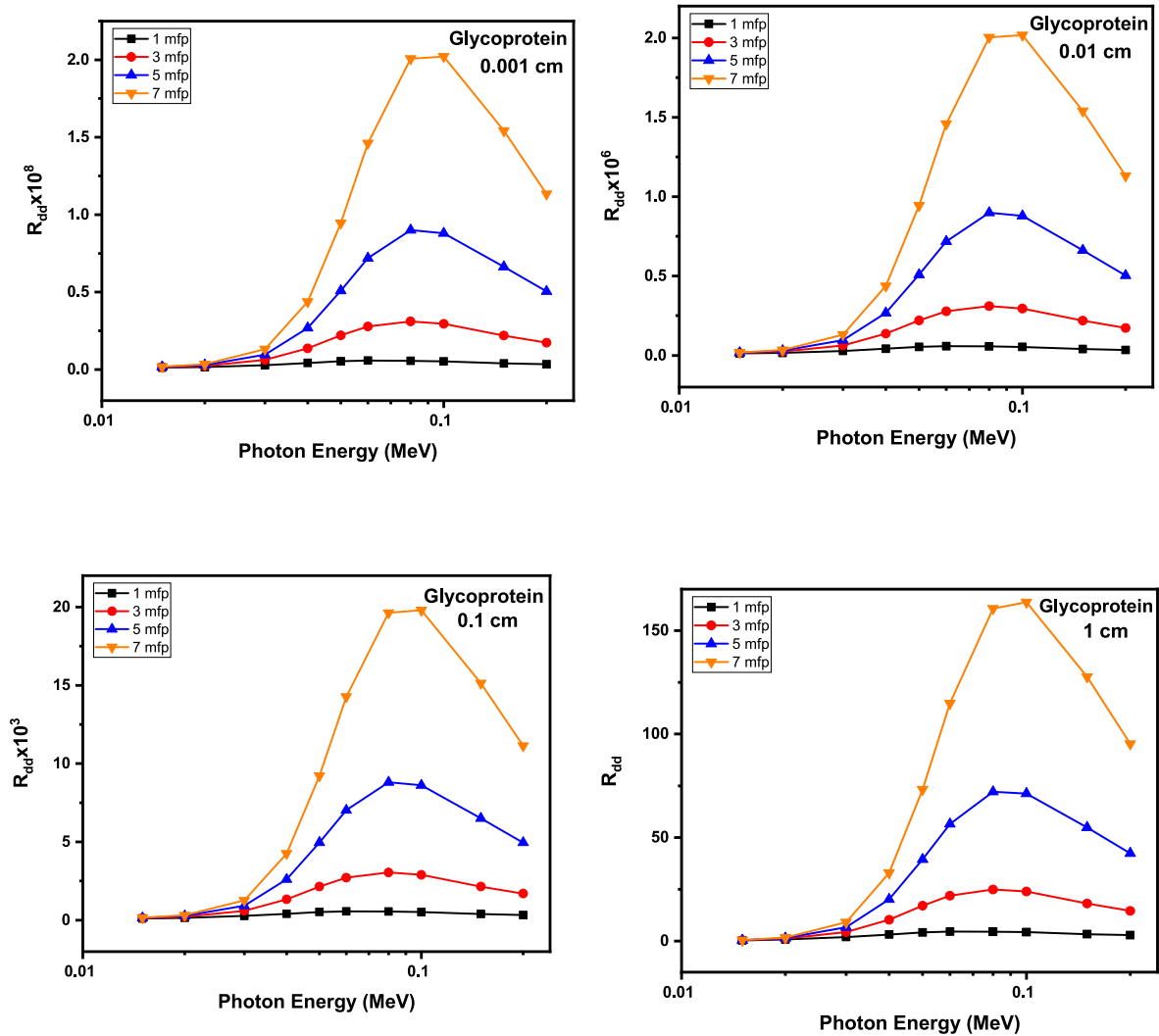
Fig. 9. Relative dose distribution values as a function of photon energy at different penetration depth (MFP) and distance (cm) of Glycoprotein layer.

gamma-ray intensities, as well as the attenuation coefficient of the target shield with a slice thickness of x. The attenuation of photons is given by the fourth equation above, in which the MAC values (μ/ρ) and W_i the weight fractions of the investigated samples. (Kara et al. 2020).

The mean free path (MFP) shows the average aperture that the wave can move without any interaction along the path inside the virus layers (Kilicoglu et al., 2021), (Alothman et al., 2021).

$$MFP = (1 / \mu) \tag{5}$$

Energy Absorption Build-up Factor (EABF) and Exposure Build-up Factor (EBF) are two other significant equations (EBF). These two parameters can be used to show the motion of uncollided/unscattered photons on the matter. The G-P approach, which is an interpolation method using the equivalent atomic number (Z_{eq}) below with the given formula, is one of the estimation methods to simulate both EABF and EBF (Kilicoglu 2019).

$$B(E,x) = 1 + \frac{b-1}{K-1}(K^x - 1) \text{ for } K \neq 1 \tag{6}$$

$$B(E,x) = 1 + (b-1)x \text{ for } K = 1 \tag{7}$$

where K (E, x) (the photon dose multiplication factor) and b (the buildup factor corresponding to 1 MFP) are derived from the following equation (Kara et al., 2020):

$$K(E,x) = cx^a + d\frac{tanh\left(\frac{x}{X_k} - 2\right) - tanh(-2)}{1 - tanh(-2)} \text{ for } x \leq 40 \, mfp \tag{8}$$

The following equation can be used to measure the relative dose distribution (RDD) at a distance x (Kilicoglu and Tekin 2020):

$$RDD = \frac{exp(-\mu x)(EBF)}{x^2} \tag{9}$$

3. Results and discussion

Simulation of radiation effects in SARS-CoV-2 is interesting for many reasons. Here, we analyze the potential use of ionizing radiation for virus inactivation in radiopharmaceutical administration. As with other chemical agents, conventional inactivation can provide by using radiopharmaceuticals which are containing gamma rays. Theydamage the membrane proteins, whereas ideally, an inactivated virus with intact membrane parts would elicit the most effective response. Here, we show that when radiopharmaceuticals containing gamma rays are used, the situation of glycoprotein and lipid layers of virus membrane is observed or SARS-CoV-2. The chemical composition of coronavirus is listed in Table 1, along with densities and weight fractions of the glycoprotein and lipid layers of the virus membrane.

The MATLAB code results are compared to results deriving from the WinXCOM computer program. The data derived from the comparison of
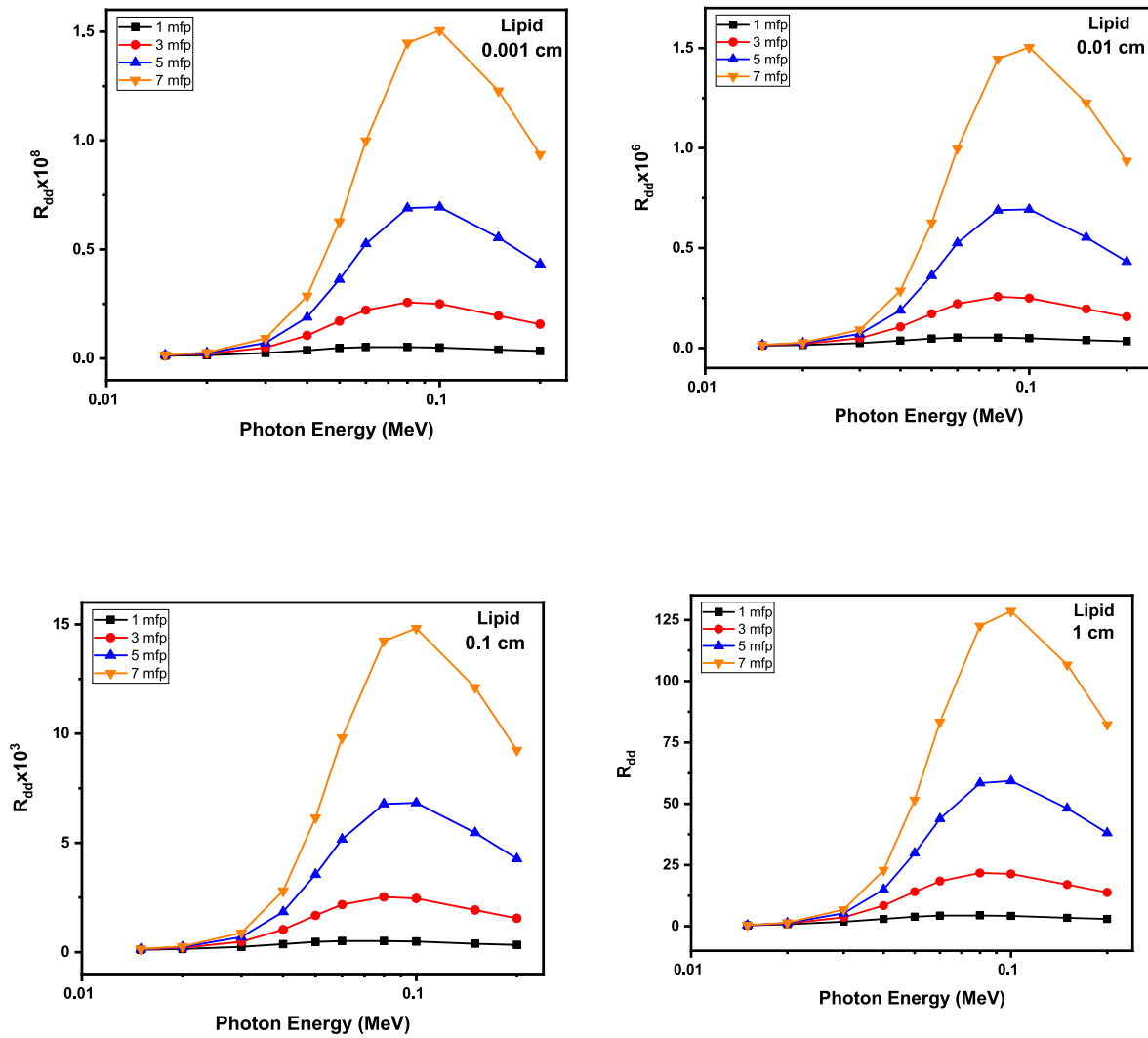
Fig. 10. Relative dose distribution values as a function of photon energy at different penetration depth (MFP) and distance (cm) of the Lipid layer.
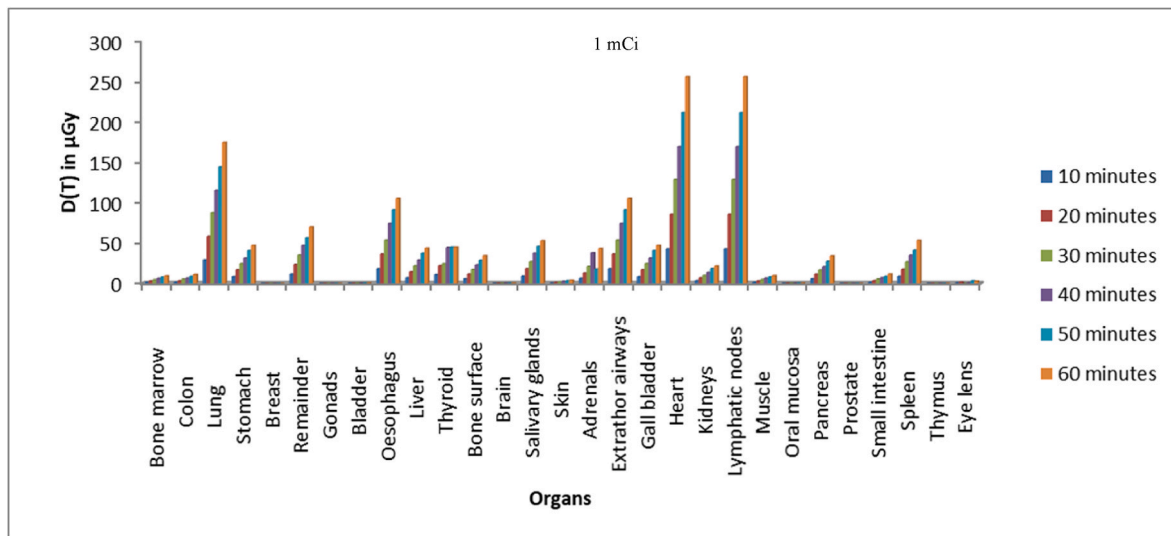

Fig. 11a. Estimation of Absorbed Organ Dose calculations for 1 mCi on Tc-99.
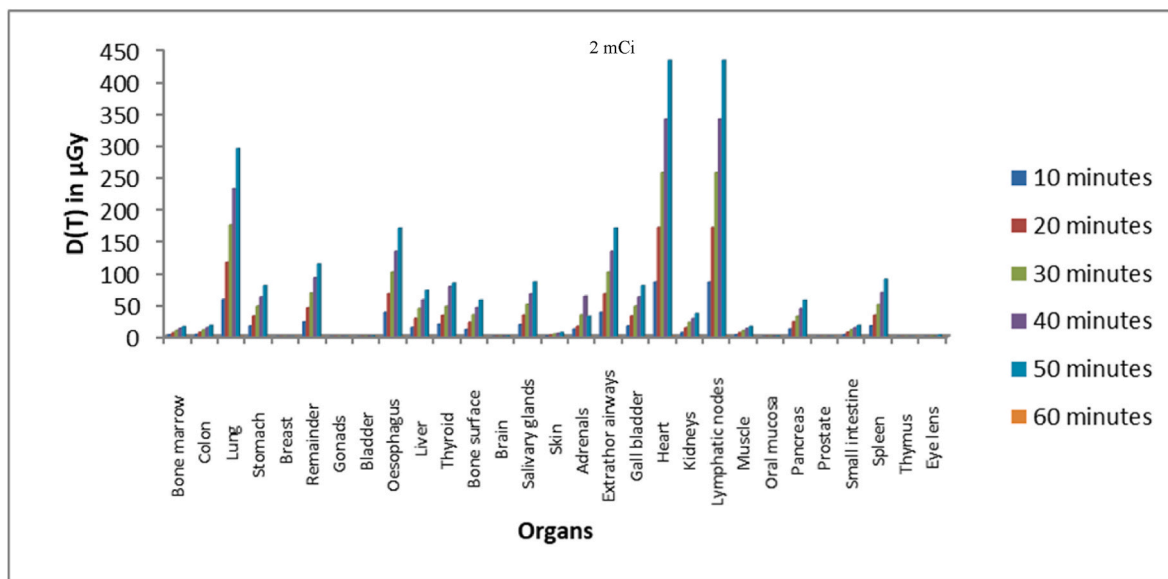
Fig. 11b. Estimation of Absorbed Organ Dose calculations for 2 mCi on Tc-99.
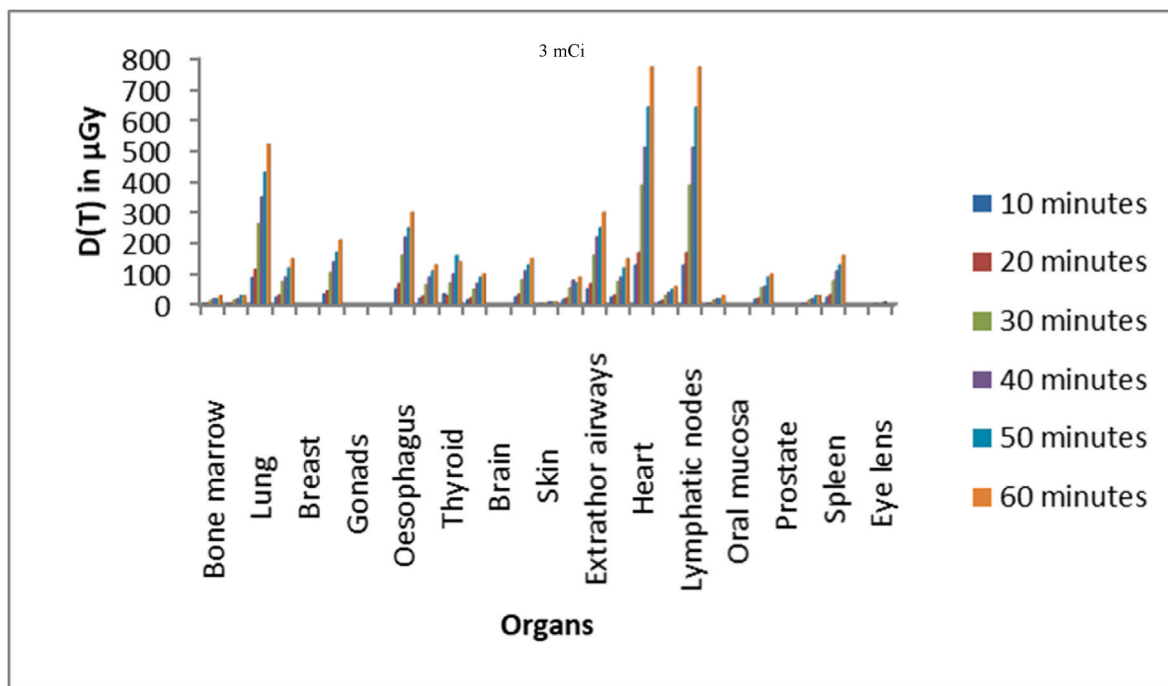

Fig. 11c. Estimation of Absorbed Organ Dose calculations for 3 mCi on Tc-99.

the results of MATLAB code and WinXCOM calculations are reported in Table 2. There is no major difference between the results of the MATLAB simulation and these samples which were started and finished at 0.015–0.2 MeV energy levels. As can be seen in the table, the results indicated that the MAC values derived from MATLAB code are in agreement with those obtained from the WinXCOM program. The deviation between the results has been determined in Table 2.

The Linear Attenuation Coefficients (LAC) values were determined by using the WinxCOM program at the energy range from 0.015 to 0.2 MeV. The findings were outlined in Fig. 4. From the figure, LAC values are highly correlated to the applied energy and the chemical properties of the GlycoProtein and Lipid layers. While the applied energy increases by up to 0.2 MeV, the LAC values show a decreasing rate, which is recorded in Fig. 4. LAC values of GlycoProtein were higher than Lipid

among the layers of the investigated virus. Results indicate that attenuation properties in low-energy regions were higher for each type of layer.

Fig. 5 displays the change in mass attenuation coefficients (MAC) in relation to incident photon energy. As the energy of the incident photons increases, the MAC values decrease. However, practically at all photon energy, the obtained mass attenuation coefficients changed slightly. In the intermediate energy range, where Compton scattering is active, MAC values vary considerably. The pair production process is dominant for energies greater than 0.15 MeV, and the MAC values are becoming approximately constant.

The term mean free path (MFP) is an important factor for measuring the average radiation distance within the material environment. The MFP values for the layers being studied were identified in Fig. 6. The
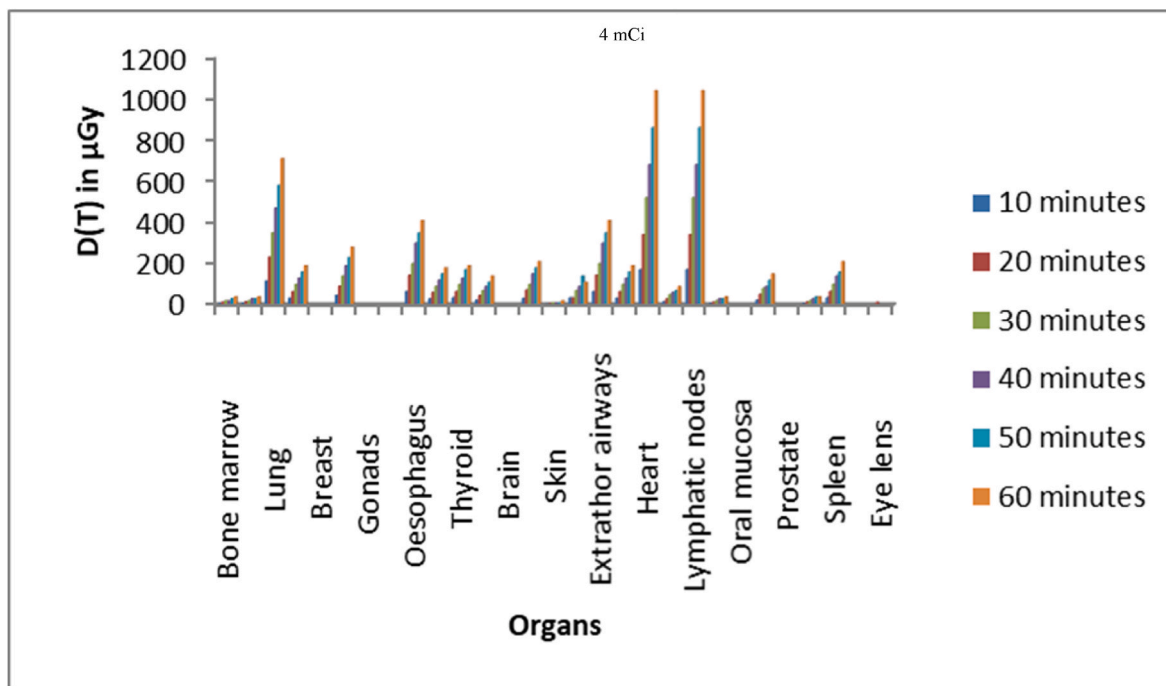
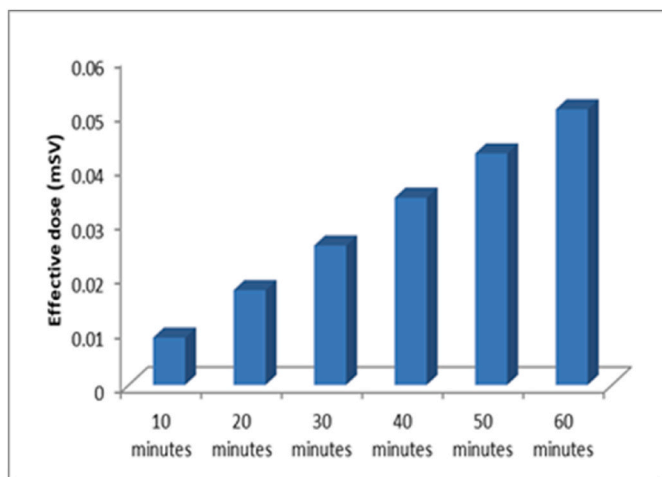**Fig. 11d.** Estimation of Absorbed Organ Dose calculations for 4 mCi on Tc-99.

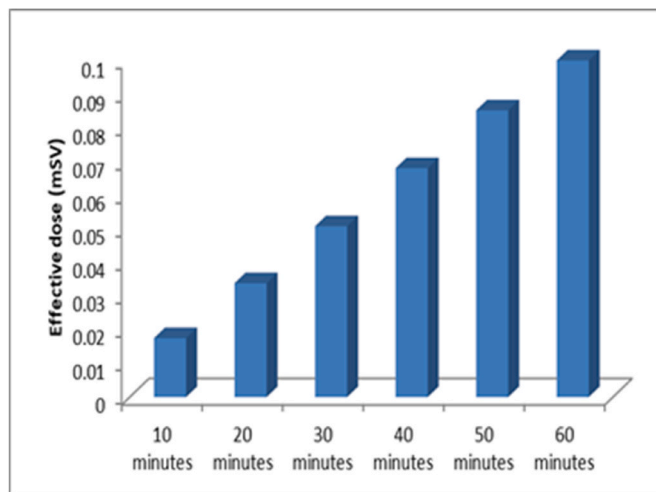**Fig. 12a.** Effective Dose calculations for 1 mCi on Tc-99.

Fig. 12b. Effective Dose calculations for 2 mCi on Tc-99.

mean free path (MFP) values of the lipid and glycoprotein layers were calculated in the range of photon energies from 0.015 to 0.2 MeV using the lineer attenuation coefficients. Fig. 6 displayed the outcomes that were obtained. As is evident in Fig. 6, the glycoprotein layer was recorded with the lowest MFP values throughout all energy levels. The MFP and linear attenuation coefficient connection may be used to describe this situation.

The values of the energy absorption build-up factor (EABF) and the exposure build-up factor (EBF) were important when selecting a replacement composite material for a particular energy region instead of a component. As such, EABF and EBF were essential for determining the material's absorption. In this study, the values of EBF-EABF were calculated using the G-P fitting approach, which is a common method used by various investigators. For measurement, the penetration depth is 1-2-3-4-5-6-7 MFP, respectively. Fig. 7 and Fig. 8 list the EBF-EABF values for the GlycoProtein and Lipid layers in the energy levels up to 0.2 MeV.

The three interactions taking place between energy and matter were the photoelectric effect, Compton scattering, and pair production. The photoelectric effect occurs when electrons are released by matter while they are exposed to electromagnetic radiation. Photoelectric effects occur in low-energy regions yielding an increasing rate of EBF and EABF with an inverse relation to $E^{3.5}$. With the rising energy, the EBF-EABF values decrease after reaching their peak at 0.1 MeV. Compton scattering is the result of a high-energy photon emerging in the intermediate energy region, leading to higher EBF-EABF values due to multiple dispersion processes. Pair production is a direct conversion of the energy of radiance into matter. As such the gamma-ray is converted into the matter in the form of a negatively and positively charged pair of electrons (negatron and positron). Pair production occurs only for gamma-rays of high energy producing a lower EAB-EABF. With a maximum value of Z_{eq}, the lipid layer is the smallest possible EBF-EABF factor among the studied layers. Figs. 7–8 shows that since the higher energy
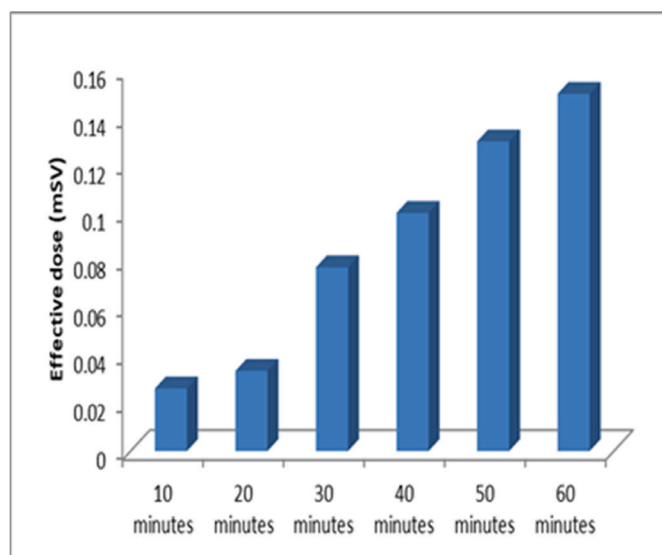
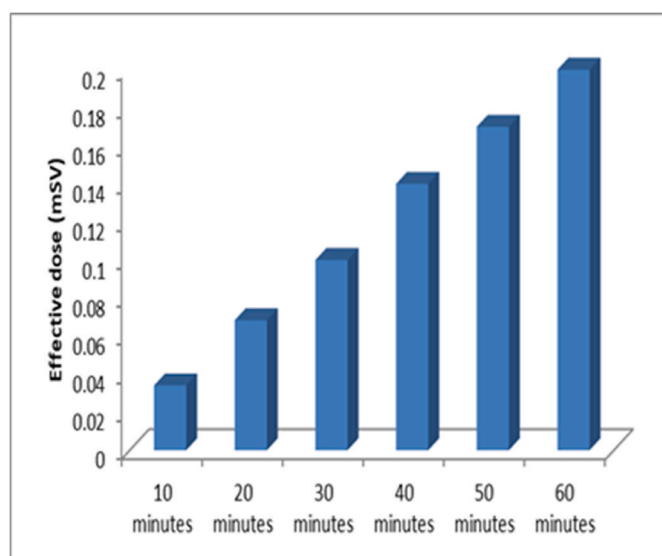**Fig. 12c.** Effective Dose calculations for 3 mCi on Tc-99.

Fig. 12d. Effective Dose calculations for 4 mCi on Tc-99.

penetrations move through the substance, higher EBF-EABF values can be seen in the energy from 0.015 MeV to 0.2 MeV and up to 7 MFP. Chemical properties were considered to have major effects on both the EBF and EABF. As can be seen in Figss. 7–8, at low energies, the lipid layer has the lowest EBF-EABF values. Despite decreasing Z_{eq} of all the layers examined, the EABF and EBF values were found to rise. There is an inverse relation between Z_{eq} and EBF-EABF values.

Vis-à vis changing energies, the variation of EBF and EABF values for the GlycoProtein and Lipid layers were reported in Figs. 7 and 8. Thanks to the K absorption edge of Sulfur and Phosphorus an abrupt peak was in this region in the low region between 0.015 and 0.1 MeV and decreases swiftly after 0.1 MeV. Here, EBF-EABF values get to the minimum levels for all investigated layers. In the 0.015–0.1 MeV, EBF and EABF incrementally rise and sharply decrease after 0.1 MeV. Making the minimum Z_{eq} glycoprotein possess the largest EBF-EABF while the maximum Z_{eq} and the smallest EBF-EABF yield the lipid layer. In a substance, a high value of Z_{eq} means it was a good radiation absorber. For high penetration depths (5–7 MFP), the EBF-EABF values display a growing pattern once again. The EBF and EABF values were decreased by increasing the

percentage of phosphorus in the lipid layer.The smaller EBF-EABF means better radiation attenuation properties. Therefore, in terms of radiation attenuation, we can conclude that the Lipid layer has a greater value than the Glycoprotein layer. The lipid layer, with the maximum value of Z_{eq} virus among the layers investigated, reached the smallest EABF-EBF as the layer of Glycoprotein, with the minimum value of Z_{eq}, reaching the largest EBF-EABF. A Relative Dose Distribution (RDD) quantitative assessment method was a calculation of the distance x to the EBF values. Variations of the RDD have been used as a distance (x) attribute for different virus layers. Figs. 9 and 10 shows the difference in the relative dose distribution of the layers of Glycoprotein and Lipid at penetration depths of 1, 3, 5, and 7 MFP for similar event energies up to 0.2 MeV and different distances up to 1 cm.

As seen in those figures, the RDD values increase to maturity depending on the depth of penetration and chemical composition of the samples. In both tests, as photon energy rises to 0.1 MeV, the RDD values increase rapidly. Increases in photon energy often help to reduce.

RDD values. Measurements of RDD around point gamma-ray emitters are important for clinical dosimetry.

Medical Internal Radiation Dosimetry (MIRD) method was used for absorbed organs and effective doses. The values of the MIRD were shown in the graphic in Fig. 11(a–d) and Fig. 12(a–d).

Since there was no good dosimetry method in the absence of high spatial resolution of molecular imaging devices, and calculations remain mostly theoretical, the MIRD method was an important aspect. The Monte Carlo Method was also software for making predictions in number of applications including medical doses. Medical dose and MIRD formulation are often used for dosimetry examinations in clinical applications. The MIRD method was based on the calculation of the dose based on the standard size of the human body and its organ models. In this method, the amount of absorbed dose in the target organs was calculated according to radioactivity in the source organs. In this regard, the interaction of the virus and radiopharmaceuticals containing gamma radiation emitter in the lungs and peripheral organs was evaluated using Monte Carlo Simulation which has drawn attention as an emerging technique for developing new drugs for Covid-19.

In addition, the Monte Carlo Simulation technique can be combined with two approaches which allow simulation of 'virtual' patients, who have virtual virus inactivation and administration of radiopharmaceutical containing gamma radiation emitter. Considering the contribution of simulation studies, they are valuable in terms of time and cost-effectiveness. We, therefore, tested the Monte Carlo technique in the pre-phase phase of our study to contribute to experimental or clinical research studies.

The SARS-CoV-2 virus enters lung cells by binding to ACE2. With the colonization of SARS-CoV-2 in the lung tissue, viral pneumonia develops and causes respiratory failure. Tc-99m MAA, (macro aggregated albumin) which is one of the technetium radiopharmaceuticals used in lung perfusion imaging, given at this point will allow low-dose gamma radiation to be applied by binding to the lung tissue. According to our results, Tc-99m MAA administration can be useful to accomplish viral inactivation in the infection site. While the literature does not have enough information about SARS-Cov2, different amounts of gamma-ray radiation emitter have been shown to achieve a reduction in virus burden, including single-stranded RNA viruses. These results agree with our findings (Sullivan et al., 1971; Thomas et al., 1981; Cramer et al., 2020).

4. Conclusion

The ongoing Covid-19 pandemic is caused by severe acute respiratory syndrome-2 known as coronavirus. The radiopharmaceuticals for Covid-19 have turned out to be an important topic in virology inactivation studies. This study offers Monte Carlo Simulation for interaction radiopharmaceuticals and virus inactivation as a pre-phase stage inactivation for Covid-19 disease as well as the analyses of other related

concepts such as the Nuclear Medicine MIRD method, and gamma radiation emitters attenuation properties, which are helpful in terms of determining the relative dose distributions.

Our findings indicate that measurements of RDD around point gamma-ray emitters are important for clinical dosimetry. Besides, the spike glycoprotein and membrane lipid layer of Covid-19 can be affected by gamma radiation emitter administration. In conclusion, radiopharmaceuticals containing gamma radiation emitters can be promising agents for the inactivation of Covid-19. In particular, gamma-ray radiation destroyed the spike glycoprotein and membrane lipid layer of Covid-19. In this case, since there is no structure left to interact with the ACE-2 receptors which are used for the virus, it will not be able to penetrate the cell. The interaction of radiopharmaceuticals with coronavirus may prevent the virus from settling in the target tissue of the lung at the onset of infection.

CRediT authorship contribution statement

Ozge Kilicoglu: Methodology, Software, Visualization, Writing – original draft, Writing – review & editing. **Umit Kara:** Visualization, Investigation. **Emre Ozgenc:** Writing – review & editing, Validation. **Evren Gundogdu:** Writing – review & editing, Validation.

Declaration of competing interest

The authors declare that they have no known competing financial interests or personal relationships that could have appeared to influence the work reported in this paper.

Data availability

No data was used for the research described in the article.

Acknowledgment

None.

References

Alothman, M.A., Alrowaili, Z.A., Al-Baradi, A.M., Kilicoglu, O., Mutuwong, C., Al-Buriahi, M.S., 2021. Elastic properties and radiation shielding ability of ZnO–P2O5/B2O3 glass system. J. Mater. Sci. Mater. Electron. 32 (14), 19203–19217. https://doi.org/10.1007/s10854-021-06442-z.

Ameri, A., Ameri, P., Rahnama, N., Mokhtari, M., Sedaghat, M., Hadavand, F., Bozorgmehr, R., Haghighi, M., Taghizadeh-Hesary, F., 2021. Low-dose whole-lung irradiation for COVID-19 pneumonia: final results of a pilot study. Int. J. Radiat. Oncol. Biol. Phys. 109 (4), 859–866. https://doi.org/10.1016/j.ijrobp.2020.11.065.

Berger, M.J., Hubbell, J.H., Seltzer, S.M., Chang, J., Coursey, J.S., Sukumar, R., Zucker, D.S., Olsen, K., et al., 2010. XCOM: photon cross sections database (NBSIR 87-3597): national institute of standards and technology. https://doi.org/10.18434/T48G6X. NIST, PML, Radiation Physics Division.

Bolch, W.E., Jokisch, D., Zankl, M., Eckerman, K.F., Fell, T., Manger, R., Endo, A., Hunt, J., Kim, K.P., Petoussi-Henss, N., 2016. ICRP publication 133: the ICRP computational framework for internal dose assessment for reference adults: specific absorbed fractions. Ann. ICRP 45 (2), 5–73.

Channappanavar, R., Perlman, S., 2017. Pathogenic human coronavirus infections: causes and consequences of cytokine storm and immunopathology. In: Semin Immunopathol, vol. 39. Springer, pp. 529–539 [place unknown].

Cramer, A., Tian, E., Sherryl, H.Y., Galanek, M., Lamere, E., Li, J., Gupta, R., Short, M.P., 2020. Disposable N95 masks pass qualitative fit-test but have decreased filtration efficiency after cobalt-60 gamma irradiation. medRxiv.

Eckerman, K., 2008. Nuclear decay data for dosimetric calculations. ICRP Publication 107. Ann. ICRP 38, 7–96.

Gerward, L., Guilbert, N., Jensen, K.B., Levring, H., 2004. WinXCom—a program for calculating X-ray attenuation coefficients. Radiat. Phys. Chem. 71 (3–4), 653–654.

Gheblawi, M., Wang, K., Viveiros, A., Nguyen, Q., Zhong, J.-C., Turner, A.J., Raizada, M. K., Grant, M.B., Oudit, G.Y., 2020. Angiotensin-converting enzyme 2: SARS-CoV-2 receptor and regulator of the renin-angiotensin system: celebrating the 20th anniversary of the discovery of ACE2. Circ. Res. 126 (10), 1456–1474.

Gutfilen, B., Valentini, G., 2014. Radiopharmaceuticals in nuclear medicine: recent developments for SPECT and PET studies. BioMed Res. Int. 2014.

Jain, V., Berman, A.T., 2018. Radiation pneumonitis: old problem, new tricks. Cancers 10 (7). https://doi.org/10.3390/cancers10070222.

Kara, U., Kilicoglu, O., Ersoy, S., 2020a. Structural and gamma-ray attenuation coefficients of different OAD films for nuclear medicine applications. Radiat. Phys. Chem. 172 https://doi.org/10.1016/j.radphyschem.2020.108785.

Kara, U., Kilicoglu, O., Karaibrahimoglu, A., Cavdarli, K., Ince, F., 2020b. Radiation attenuation properties of removable partial dentures (RPD). Mater. Chem. Phys. 253 https://doi.org/10.1016/j.matchemphys.2020.123301.

Kilicoglu, O., 2019. Characterization of copper oxide and cobalt oxide substituted bioactive glasses for gamma and neutron shielding applications. Ceram. Int. 45 (17, B), 23619–23631. https://doi.org/10.1016/j.ceramint.2019.08.073.

Kilicoglu, O., Kara, U., Inanc, I., 2021. The impact of polymer additive for N95 masks on gamma-ray attenuation properties. Mater. Chem. Phys. 260, 124093.

Kilicoglu, O., Tekin, H.O., 2020. Bioactive glasses with TiO2 additive: behavior characterization against nuclear radiation and determination of buildup factors. Ceram. Int. 46 (8), 10779–10787.

Kilicoglu, O., Mehmetcik, H., 2021. Science mapping for radiation shielding research. Radiat. Phys. Chem. 189, 109721 https://doi.org/10.1016/j.radphyschem.2021.109721.

Kirkby, C., Mackenzie, M., 2020. Is low dose radiation therapy a potential treatment for COVID-19 pneumonia? Radiother Oncol. J. Eur. Soc. Ther. Radiol. Oncol. 147, 221. https://doi.org/10.1016/j.radonc.2020.04.004.

Lederman, M.M., Cannon, P.M., Currier, J.S., June, C.H., Kiem, H.-P., Kuritzkes, D.R., Lewin, S.R., Margolis, D.M., McCune, J.M., Mellors, J.W., 2016. A cure for HIV infection:"not in my lifetime" or "just around the corner". Pathog Immun. 1 (1), 154.

Little, M.P., Zhang, W., van Dusen, R., Hamada, N., 2021. Pneumonia after bacterial or viral infection preceded or followed by radiation exposure: a reanalysis of older radiobiologic data and implications for low-dose radiation therapy for coronavirus disease 2019 pneumonia. Int. J. Radiat. Oncol. Biol. Phys. 109 (4), 849–858. https://doi.org/10.1016/j.ijrobp.2020.09.052.

Lyra, M., Ploussi, A., Georgantzoglou, A., Ionescu, P.C., 2011. Matlab as a tool in nuclear medicine image processing. In: MATLAB- Ubiquitous Tool Pract Eng. InTech, pp. 477–500 [place unknown].

Masur, H., Brooks, J.T., Benson, C.A., Holmes, K.K., Pau, A.K., Kaplan, J.E., 2014. Prevention and treatment of opportunistic infections in HIV-infected adults and adolescents: updated guidelines from the centers for disease control and prevention, national institutes of health, and HIV medicine association of the infectious diseases society of America. Clin. Infect. Dis. 58 (9), 1308–1311.

Mattsson, S., Johansson, L., Leide Svegborn, S., Liniecki, J., Noßke, D., Riklund, K.Å., et al., 2015. ICRP publication 128: radiation dose to patients from radiopharmaceuticals: a compendium of current information related to frequently used substances. Ann. ICRP 44 (2_Suppl. l), 7–321.

Mazzone, H.M., 1998. CRC Handbook of Viruses: Mass-Molecular Weight Values and Related Properties. CRC Press [place unknown].

Mettler Jr., F.A., Guiberteau, M.J., 2012. Essentials of Nuclear Medicine Imaging: Expert Consult-Online and Print. Elsevier Health Sciences [place unknown].

Miyoshi, T., Lönnfors, M., Slotte, J.P., Kato, S., 2014. A detailed analysis of partial molecular volumes in DPPC/cholesterol binary bilayers. Biochem. Biophy. Acta. Biomember. 1838 (12), 3069–3077.

Nasir, A., Agrawal, D., Pathak, J., Theodoulou, I., 2021. Low-dose X-ray therapy for COVID-19: lessons from the past. Br. J. Radiol. 94 (1117), 20200581 https://doi.org/10.1259/bjr.20200581.

Oppenheimer, A., 1943. Roentgen therapy of interstitial pneumonia. J. Pediatr. 23 (5), 534–538. https://doi.org/10.1016/S0022-3476(43)80256-0.

Padilla-Sanchez, V., 2020. In silico analysis of SARS-CoV-2 spike glycoprotein and insights into antibody binding. Res Ideas Outcome. 6, e55281.

Prasanna, P.G., Woloschak, G.E., DiCarlo, A.L., Buchsbaum, J.C., Schaue, D., Chakravarti, A., Cucinotta, F.A., Formenti, S.C., Guha, C., Hu, D.J., et al., 2020. Low-dose radiation therapy (LDRT) for COVID-19: benefits or risks? Radiat. Res. 194 (5), 452–464. https://doi.org/10.1667/RADE-20-00211.1.

Qin, Z., 2015. Recent advances of injectable radiopharmaceuticals for nuclear imaging and therapy: a new era in nuclear medicine. Mater. Technol. 30 (Suppl. 8), B250–B255.

Salomaa, S., Bouffler, S.D., Atkinson, M.J., Cardis, E., Hamada, N., 2020. Is there any supportive evidence for low dose radiotherapy for COVID-19 pneumonia? Int. J. Radiat. Biol. 96 (10), 1228–1235. https://doi.org/10.1080/09553002.2020.1786609.

Sullivan, R., Fassolitis, A.C., Larkin, E.P., Read, R.B., Peeler, J.T., 1971. Inactivation of thirty viruses by gamma radiation. Appl. Microbiol. 22 (1), 61–65.

Terán, M., Savio, E., Paolino, A., Frier, M., 2005. Hydrophilic and lipophilic radiopharmaceuticals as tracers in pharmaceutical development: in vitro–In vivo studies. BMC Nucl. Med. 5 (1), 1–8.

Thomas, F.C., Davies, A.G., Dulac, Gc, Willis, N.G., Papp-Vid, G., Girard, A., 1981. Gamma ray inactivation of some animal viruses. Can. J. Comp. Med. 45 (4), 397.

Vardhan, S., Sahoo, S.K., 2020. Searching Inhibitors for Three Important Proteins of COVID-19 through Molecular Docking Studies. ArXiv Prepr ArXiv200408095.

Wan, Y., Shang, J., Graham, R., Baric, R.S., Li, F., 2020. Receptor recognition by the novel coronavirus from Wuhan: an analysis based on decade-long structural studies of SARS coronavirus. J. Virol. 94 (7).

Zhou, P., Yang, X.-L., Wang, X.-G., Hu, B., Zhang, L., Zhang, W., Si, H.-R., Zhu, Y., Li, B., Huang, C.-L., 2020. A pneumonia outbreak associated with a new coronavirus of probable bat origin. Nature 579 (7798), 270–273.

Ziessman, H.A., O'Malley, J.P., 2013. Nuclear Medicine: the Requisites. Elsevier Health Sciences [place unknown].